Self-Assembly of H-Shaped Block Copolymers

Yang Cong, Binyao Li, and Yanchun Han*

State Key Laboratory of Polymer Physics and Chemistry, Changchun Institute of Applied Chemistry, Chinese Academy of Sciences, Graduate School of the Chinese Academy of Sciences, 5625 Renmin Street, Changchun 130022, P.R. China

Yugang Li and Caiyuan Pan

Department of Polymer Science and Engineering, University of Science and Technology of China, Hefei 230026, P.R. China

Received July 18, 2005; Revised Manuscript Received September 7, 2005

ABSTRACT: We have systematically studied the effect of the solvent nature on the self-assembly of H-shaped block copolymers with a poly(ethylene glycol) backbone and polystyrene branches, i.e., $(PS)_2PEG(PS)_2$. Two copolymers with different molecular weights (MW) and compositions, copolymer **1** and copolymer **2**, were used, where copolymer **2** has a higher MW and higher PEG fraction than those of copolymer **1**. In nominally neutral (nonselective) solvents, it is found that very subtle variation in the solvent affinity can remarkably influence the morphologies of the films spin-coated from the corresponding solutions. For example, as the solvent was changed from PS-affinitive to PEG-affinitive, the films of copolymer **1** changed from a disordered state into PEG cylinders. In contrast, the films of copolymer **2** changed from wormlike patterns into PEG spheres. Besides, the surface morphologies also showed some dependence on the solution concentration: with decreasing concentration, the PEG cylinders were changed into PEG spheres and a disordered state. In PEG-selective solvent (e.g., acetonitrile), copolymer **2** formed typical spherical micelles. In contrast, copolymer **1** formed a mixture of spheres and cylinders, which could be transformed into vesicles and lamellae upon dilution. The polymer−solvent interactions and their effects on the copolymer chain conformation are discussed.

1. Introduction

During the past decades, intensive studies have been performed on the self-assembly of block copolymers in solutions, focusing mainly on linear diblock and triblock copolymers. The self-assembly of block copolymers in solutions is more complicated than that in melts due to the additional role played by the solvent. The phase behavior depends strongly on the polymer−solvent interaction parameter (χ_{P-S}), besides the volume fraction of the minority block (f), the total polymerization degree (N), the polymer concentration (φ), and the Flory−Huggins interaction parameter between the A and B blocks (χ_{AB}).[1] In concentrated solutions, neutral solvents can decrease the A/B interaction parameter (χ_{AB}) by a factor of concentration (φ) according to the dilution approximation.[2] For dilute solutions of neutral solvents, the effective A/B interaction parameter ($\chi_{eff} = \varphi\chi_{AB}$) should be much lower.[3] In other words, neutral solvents can shield the unfavorable contact of the blocks. Due to the industrial and scientific significance,[4] increasing interest has been arising on the self-assembly of block copolymers in selective solvents. In selective solvents, block copolymers can self-assemble to form micelles or aggregates of various geometries. The geometry of the aggregates is a result of the balance of three factors: the stretching of the core-forming blocks, the repulsive interactions of the corona chains, and the interfacial tension between the micelle core and the solvent.[5] This competition can be adjusted by a number of factors such as copolymer composition,[6] copolymer concentration,[7] solvent nature,[8] temperature,[9−11] time,[10] preparation methods,[11] and the presence of additives.[12]

The development of new synthetic methods[13] enables the synthesis of polymers with complicated architectures such as graft,[14] star,[15] gradient,[16] comb,[17] dendritic,[18] cyclic,[19] and tadpole-shaped polymers.[20] These architectured polymers show some unique properties in bulk and solution, which may promise profound applications in many fields[21] and inspire some new aspects in fundamental research. In this work, we investigate the self-assembly of H-shaped copolymers in dilute solutions.

Since the first synthesis of H-shaped polystyrenes (PSs) by Roovers and Toporowski in 1981,[22] a few H-shaped homopolymers (e.g., polyisoprene (PI)[23] and polybutadiene (PB)[24]), copolymers (with a polyisoprene backbone and polystyrene branches (S_2IS_2)),[21] super-H-shaped, and π-shaped copolymers[21,25] were synthesized. The bulk properties of these architectured polymers, including melt rheology, relaxation, and microphase-separated structure, have been investigated by small-angle neutron scattering (SANS),[26−29] molecular dynamics simulation,[30] transmission electron microscopy (TEM), and small-angle X-ray scattering (SAXS).[21,31] Gido and co-workers suggested that the morphological behavior of the H-shaped S_2IS_2 was approximately equivalent to that of the constituting block copolymer structure (e.g., $S_2((1/2)I)$).[21,31] On the other hand, the solution properties of H-shaped and super-H-shaped copolymers were studied mainly in selective solvents by SANS, static and dynamic light scattering, and viscometry. Due to the effect of the special architecture, the H-shaped copolymers were found to form micelles with lower aggregation numbers than those of the corresponding linear diblock and triblock copolymers.[32,33]

In this paper, we study the self-assembly of newly designed and synthesized H-shaped block copolymers,[34]

* To whom correspondence should be addressed. Phone: +86-431-5262175. Fax: +86-431-5262126. E-mail: ychan@ciac.jl.cn.

10.1021/ma0515679 CCC: $30.25
Published on Web 10/11/2005

Table 1. Characterization of H-shaped $(PS)_2PEG(PS)_2$ Samples[a]

no.	copolymer	$M_{n,NMR}$ (PEG)	$M_{n,NMR}$ (copolymer)	M_w/M_n (GPC)	f_{PEG} (V%)	T_c^{PEG} (°C)	T_m^{PEG} (°C)	T_g^{PEG} (°C)	T_g^{PS} (°C)
1	$(PS)_2PEG(PS)_2$	8500	46100	1.06	17.5		26.6	−54.2	77.3
2	$(PS)_2PEG(PS)_2$	27000	87800	1.10	29.4	∼10	49.2		76.2

[a] See ref 34.

$(PS)_2PEG(PS)_2$, in nominally neutral (nonselective) and selective solvents. Two copolymers with different molecular weights and compositions, copolymers **1** and **2**, are used. In nominally neutral solvents, very subtle change in the solvent affinity to a specific block, as well as the solution concentration, can remarkably influence the film morphology. In PEG-selective solvent (acetonitrile), copolymer **2** formed stable spherical micelles, while the geometry of the copolymer **1** aggregates exhibits remarkable dependence on the preparation conditions. The effect of the polymer−solvent interaction on the copolymer aggregation will be discussed.

2. Experiments

2.1. Block Copolymer Synthesis and Characterization. The H-shaped block copolymer with a poly(ethylene glycol) (PEG) backbone and polystyrene (PS) branches $(PS)_2PEG(PS)_2$ was synthesized by atom transfer radical polymerization (ATRP) of styrene at 110 °C using the multifunctional macroinitiator, 2,2-bis(methylene α-bromopropionate) propionyl terminated poly(ethylene glycol) (BMBP−PEG−BMBP), and CuBr/2,2′-bipyridine as the catalyst system. The synthesis details have been described in ref 34. Two copolymers with different molecular weights and volume fractions were obtained. The characteristics of these two copolymers are summarized in Table 1, according to ref 34. The molecular weight (MW) and molecular weight distribution (MWD) of the polymers were measured by proton nuclear magnetic resonance (^{1}H NMR, Bruker DMX-300) and gel permeation chromatography (GPC, Waters 150C), respectively. Copolymer **1** has a total number average molecular weight (M_n) of 46 100 (MWD = 1.06), with the PEG, $M_{n,NMR}$ of 8500 (MWD = 1.02). Copolymer **2** has an M_n of 87 800 (MWD = 1.10), with the PEG, $M_{n,NMR}$ of 27 000 (MWD = 1.03). Thus, the PEG volume fraction (f_{PEG}) is 0.175 for copolymer **1** and 0.294 for copolymer **2**.

The glass transition temperatures (T_g's), the PEG melting point (T_m^{PEG}), and the PEG crystallization temperature (T_c^{PEG}) of the polymers were determined by differential scanning calorimetry (DSC, Mettler-Toledo DSC-8210) at heating and cooling rates of 10 °C/min.[34] Indium and benzoic acid were used as temperature calibration standards. Copolymer **2** exhibits the melting endotherm of PEG (T_m^{PEG}) at 49.2 °C and the glass transition temperature of PS (T_g^{PS}) at 76.0 °C.[34] The decrease in the T_m^{PEG} and the T_g^{PS} compared with those of the PEG homopolymer (63 °C)[35] and PS homopolymer (100 °C)[36] is due to the incorporation of the two blocks into a block copolymer, indicating a partial phase compatibility. In copolymer **1**, with shorter PEG segments, the T_m^{PEG} decreased to 26.6 °C, and no exothermic crystallization peak for PEG was detected.[34] This might be due to an improved phase compatibility of the short PEG blocks and the dominant PS blocks. These results imply that the copolymer **2** is at an intermediate microphase-separated state and copolymer **1** is at a weak microphase-separated state.

2.2. Sample Preparation. All of the solvents, chloroform, benzene, ethyl acetate, cyclohexanone, and acetonitrile, were purchased from the Beijing Chemical Plant and were distilled before use. The silicon wafers were cleaned in a piranha solution (70/30 v/v of concentrated H_2SO_4 and 30% H_2O_2) at 90 °C for 20 min, thoroughly rinsed with deionized water, and finally blown dry with nitrogen.

The $(PS)_2PEG(PS)_2$ powders were dissolved in purified chloroform, benzene, ethyl acetate, and cyclohexanone to produce 0.5 wt % solutions in nominally neutral solvents at room temperature. Storage over 48 h was performed to achieve sufficient dissolution. For the cyclohexanone solutions, the concentration was varied from 0.7 to 0.5, 0.3, and 0.1 wt %.

The micellar solutions of copolymer **2** in (PEG-selective) acetonitrile with different concentrations (such as 0.05, 0.2, 0.5, and 1 wt %) were prepared at room temperature. In contrast, the micellar solutions of copolymer **1** in acetonitrile (with concentrations of 0.2−0.05 wt %) were produced by dissolving the powders at 100 °C in an autoclave for 5 h, since copolymer **1** cannot dissolve in acetonitrile at room temperature. After that, the autoclave was quenched in an ice bath. For comparison, copolymer **2** powders were also dissolved in acetonitrile at the same conditions. These micellar solutions were transferred into sealed vials, which were stored at 10 °C for use.

All the solutions were spin-coated onto freshly cleaned silicon wafers with 2 nm native oxide cover. The samples were immediately dried in a vacuum oven at room temperature for more than 24 h to remove the residual solvents.

2.3. Atomic Force Microscopy (AFM). The surface morphologies of all the films were characterized with an atomic force microscope (SPA300HV/SPI3800N, Seiko Instruments Inc., Japan) in tapping mode at ambient atmosphere. A silicon cantilever (spring constant ∼2 N/m and resonant frequency ∼70 kHz, Olympus Co., Japan) with an etched conical tip (radius of curvature ∼40 nm as characterized by scanning over a very sharp needle array, NT-MDT, Russia) was used for scanning. To examine the surface structures, both height and phase images were recorded. The phase contrast was believed to reflect the material composition and distribution on the surface since the phase contrast did not substantially change while we tentatively tuned the scanning conditions (e.g., set point, scan rate, scan size, etc.).[37] All analyses of the images were conducted in the integrated software.

2.4. Transmission Electron Microscopy (TEM). Transmission electron microscopy was performed on a JEM-1011 transmission electron microscope (JEOL Inc., Japan) operated at 100 kV accelerating voltage. The TEM samples were prepared by casting a drop of copolymer solution on a copper grid and quickly wicking away the excess solution with filter paper. The samples were imaged by TEM without staining due to the difference of electron density between the PEG and PS blocks.[38]

3. Results and Discussion

In the A−B block copolymer solutions, the polymer−solvent interaction parameter, χ_{A-S} and χ_{B-S}, in addition to the f, N, φ, and χ_{AB}, can significantly influence the copolymer phase behavior.[1] The polymer−solvent interaction parameter, χ_{P-S},[36] can be estimated by

$$\chi_{P-S} = V_S(\delta_S - \delta_P)^2/RT + 0.34 \quad (1)$$

where V_S is the molar volume of the solvent, R is the gas constant, T is the Kelvin temperature, and δ_S and δ_P are the solubility parameters of the solvent and polymer, respectively. The solubility parameters of PS and PEG are $\delta_{PS} = 18.6$ $(J/cm^3)^{1/2}$ and $\delta_{PEG} = 19.9$ $(J/cm^3)^{1/2}$, respectively.[36] Thus, the χ_{P-S} values for different polymer−solvent pairs at room temperature (18 °C) can be calculated according to eq 1, as listed in Table 2. According to the Flory−Huggins theory criterion, the polymer and solvent are completely miscible over the entire composition range when $\chi_{P-S} < 0.5$. Thus, chlo-

Table 2. Polymer−Solvent Interaction Parameters (χ_{P-S}) Calculated for Different Polymer−Solvent Pairs

	chloroform	benzene	ethyl acetate	cyclo-hexanone	acetonitrile
PS	0.3453	0.3415	0.3400	0.4638	1.0414
PEG	0.3668	0.3847	0.4082	0.3469	0.7579
$\Delta\chi$	0.0215	0.0432	0.0682	0.1169	0.2835

roform, benzene, ethyl acetate, and cyclohexanone are good solvents for both PS and PEG blocks. However, for a specific solvent, there is small difference between the χ_{PS-S} and χ_{PEG-S} values. Such subtle difference is concerned as the difference in the affinity of the solvent to a specific block. Namely, chloroform, benzene, and ethyl acetate have preferential affinity to PS, while cyclohexanone has preferential affinity to PEG. In contrast, acetonitrile is a selective solvent to PEG blocks.

3.1. Self-Assembly in Nominally Neutral Solvents. 3.1.1. Film Morphologies from PS-Affinitive Neutral Solvents. Figure 1 shows the morphologies of copolymer **1** films spin-coated from 0.5 wt % chloroform (Figure 1a,a′), benzene (Figure 1b,b′), and ethyl acetate (Figure 1c,c′) solutions onto the silicon substrates. The films are very flat, with the root-mean-square (rms) roughness of ~0.36 to 0.59 nm. The corresponding phase images have low phase contrast (~1.3° to 1.5°). Both height and phase images indicate that the copolymer **1** films are in a disordered state.

In contrast, patterns are observed at the surface of the films spin-coated from the 0.5 wt % solutions of copolymer **2** in chloroform, benzene, and ethyl acetate, as shown in Figure 2. In chloroform, the copolymer chains aggregate into tiny grains with the average diameter of about 20 nm, with the phase contrast of 2.8° (Figure 2a,a′). From benzene, the copolymer chains form larger aggregates, with a higher aspect ratio (the ratio of the length to the diameter of the aggregate) (~2.5 to 3) than that from chloroform (~1.2 to 1.8): the apparent average diameter slightly increases to ~22 nm (Figure 2b). Remarkably, the boundary among the aggregates becomes sharper than that in Figure 2a. The corresponding phase contrast increases to 4.1° (Figure 2b′). From the solution in ethyl acetate, the aggregates grow even larger, with the apparent average diameter of 26 nm and larger aspect ratio (~5 to 6) (Figure 2c) in

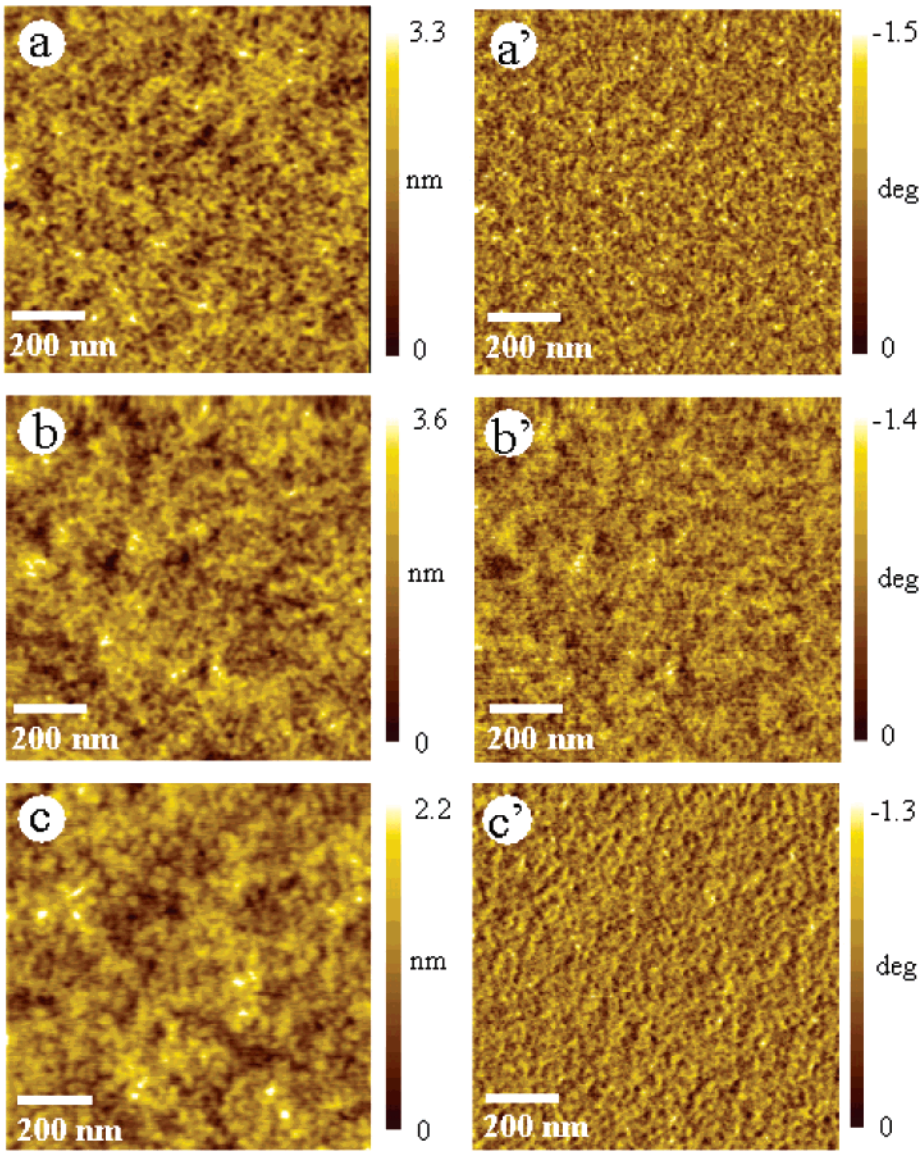

Figure 1. Tapping mode AFM height (a−c) and phase (a′−c′) images of copolymer **1** films spin-coated from 0.5 wt % (a,a′) chloroform, (b,b′) benzene, and (c,c′) ethyl acetate solutions.

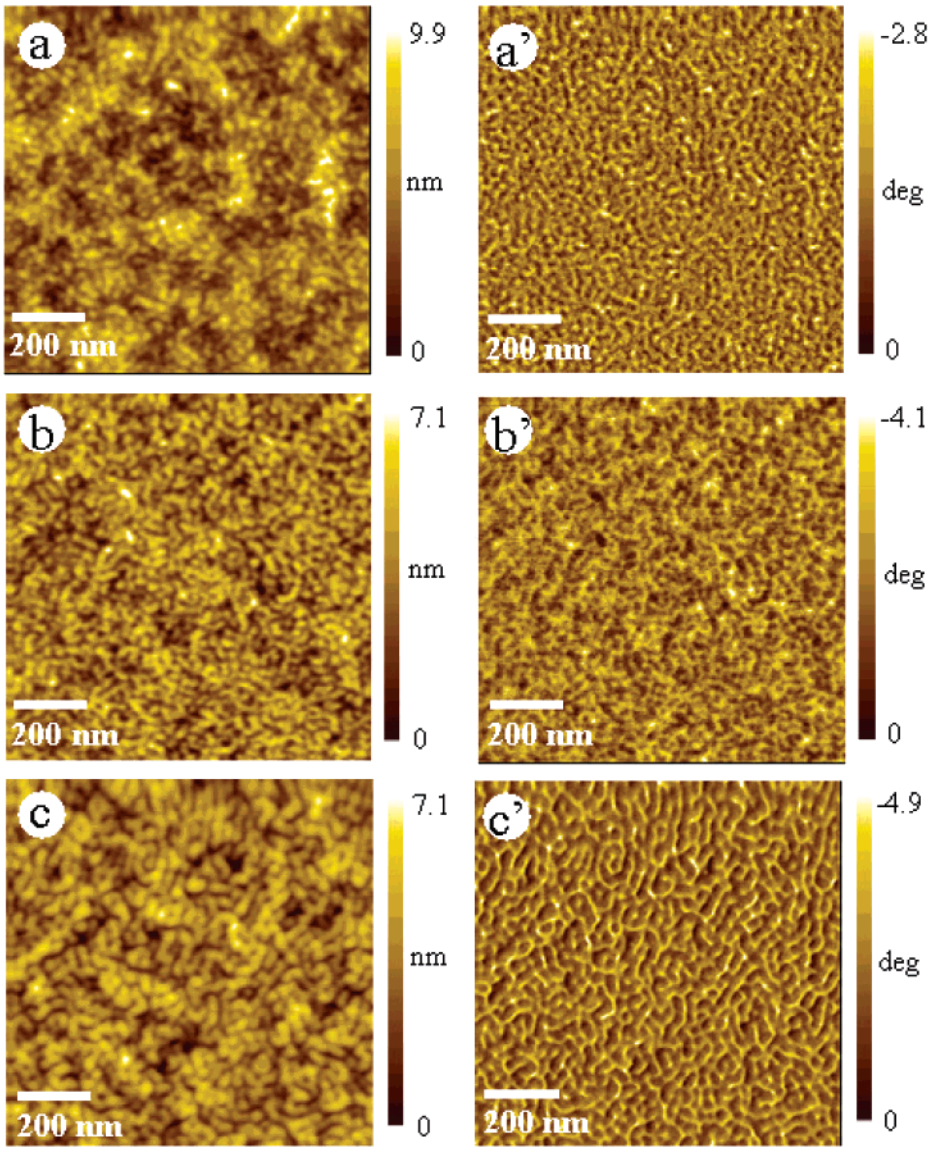

Figure 2. Tapping mode AFM height (a−c) and phase (a′−c′) images of copolymer **2** films spin-coated from 0.5 wt % (a,a′) chloroform, (b,b′) benzene, and (c,c′) ethyl acetate solutions.

comparison with those obtained from chloroform and benzene. Correspondingly, the phase contrast slightly increases to 4.9°. Clearly, the boundaries in both the height and phase images become sharper (Figure 2c′).

We carefully examined the phase images by repeated scanning of the same areas with different set points (0.7−0.95) and scan rates; the phase contrast did not change significantly. Therefore, it is reasonable to assume that the phase contrast reflects the distribution of the materials of different moduli at the film surface: the light domains correspond to soft materials which induce more phase lag of the cantilever, while the dark domains correspond to the hard materials which induce less phase lag.[37,39] Since the crystallizable PEG segments are harder than the amorphous PS, it can be deemed that the darker domains are PEG and the lighter domains are PS. That is, these wormlike patterns are PEG cylinders in a PS matrix (Figure 2).

These apparent increases in the size and the phase contrast of the copolymer **2** aggregates imply the enhancement in the phase separation between the PS and PEG blocks in the dilute solutions in these neutral solvents. Normally, neutral solvents have an effect of shielding the unfavorable contact between the unlike blocks and thus depress the segregation strength of the copolymers. However, there are no ideal neutral solvents that can equally dissolve the different polymers. The so-called neutral solvents always show some preferential affinity to one of the blocks.[40] In our work, such affinity is defined as the difference between the interaction parameters of different polymer−solvent pairs ($\Delta\chi$), which is summarized in Table 2.

The interaction parameters at room temperature (χN(18 °C)) for the copolymers **1** and **2** are 36.6 and 79.1, respectively, according to the equation by Zhu et al.[38] For copolymer **1** in these neutral solvents, it is likely that the solvent shielding effect dominates so that copolymer **1** formed disordered thin films. In contrast, copolymer **2** formed assemblies in neutral solvents. The evolution of the morphology reflects the effect of the solvent affinity on the assembling behavior of the copolymer **2** chains.

According to the χ_{P-S} and $\Delta\chi$ values in Table 2, chloroform, benzene, and ethyl acetate are slightly affinitive to the PS blocks. Thus, the PS blocks are more swollen than the PEG blocks are; there must be some

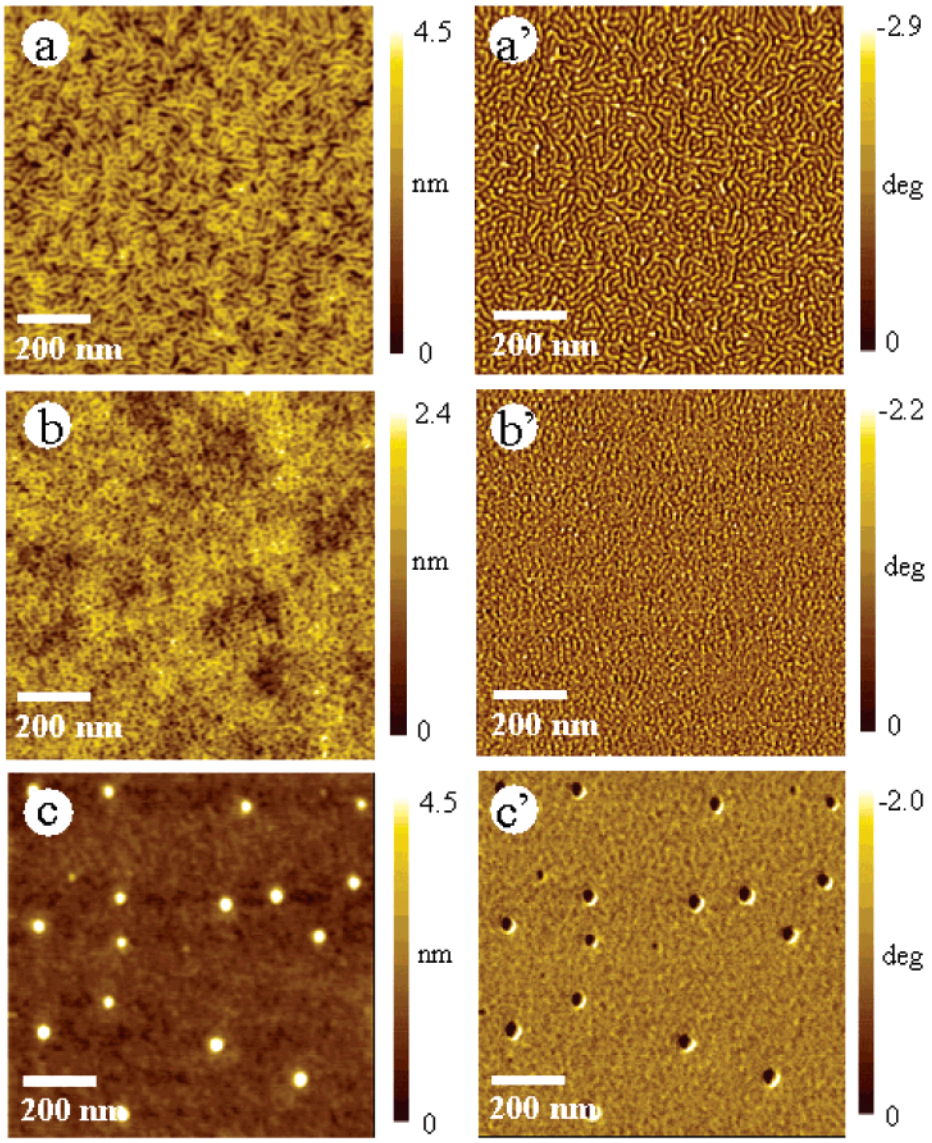

Figure 3. Tapping mode AFM height (a−c) and phase (a′−c′) images of copolymer **1** films spin-coated from (a,a′) 0.5%, (b,b′) 0.3%, and (c,c′) 0.1 wt % cyclohexanone solutions.

curvature at the PS/PEG interface and a slight difference between the blocks, which may collectively drive some specific associates of the copolymer chains in solutions.[41−43]

As the affinity to the PS blocks ($\Delta\chi$) slightly increases, such conformation difference between the PS and PEG blocks will be enlarged. Since the χ_{PS-S} slightly decreases and χ_{PEG-S} slightly increases from chloroform to benzene and ethyl acetate (Table 2), the PS chains are more swollen while the PEG blocks are more collapsed. Thus, for a given aggregation number, the repulsion between the PS chains will increase so that the PS chains are more stretched. As a result, the aggregation number will increase so that the repulsion can be relaxed. In comparison to the spherical associates, the cylindrical geometry permits a very large association number and more relaxed chain conformation and thus is favorable as the $\Delta\chi$ further increases (Figure 2c,c′). The increase in the phase contrast indicates the enhanced separation between the PS and PEG chains with the increasing $\Delta\chi$ value.

3.1.2. Film Morphologies from PEG-Affinitive Neutral Solvent. Now we present the morphologies of the thin films spin-coated from the copolymer solutions in cyclohexanone, a PEG-affinitive neutral solvent ($\chi_{PS-cyclo} = 0.4638$, $\chi_{PEG-cyclo} = 0.3469$, $\Delta\chi = 0.1169$, Table 2). Figure 3 displays the surface morphologies of the films spin-coated from the 0.5, 0.3, and 0.1 wt % copolymer **1**/cyclohexanone solutions. The film surface spin-coated from 0.5 wt % solution is featured as wormlike cylinders (Figure 3a,a′). When the solution concentration is decreased to 0.3 wt %, the structure of the wormlike cylinders is markedly weakened (Figure 3b,b′). As the concentration is decreased to 0.1 wt %, the coexistence of spheres and unimers (the underlying flat film) is observed (Figure 3c,c′). The phase contrast decreased with the decreasing concentration, implying a slight depression in the segregation strength.

Figure 4 displays the surface morphologies of the copolymer **2** films spin-coated from 0.7, 0.5, and 0.1 wt % solutions in cyclohexanone. With decreasing concentration, the surface morphology transformed from wormlike PEG cylinders in a PS matrix (Figure 4a,a′) to PEG spheres in a PS matrix (Figure 4b,b′) and the coexistence of spheres and unimers (Figure 4c,c′), where the PEG phase appears as dark domains in the phase images. Additionally, the structure in Figure 4a can be confirmed by the TEM micrograph (Figure 4d) of the

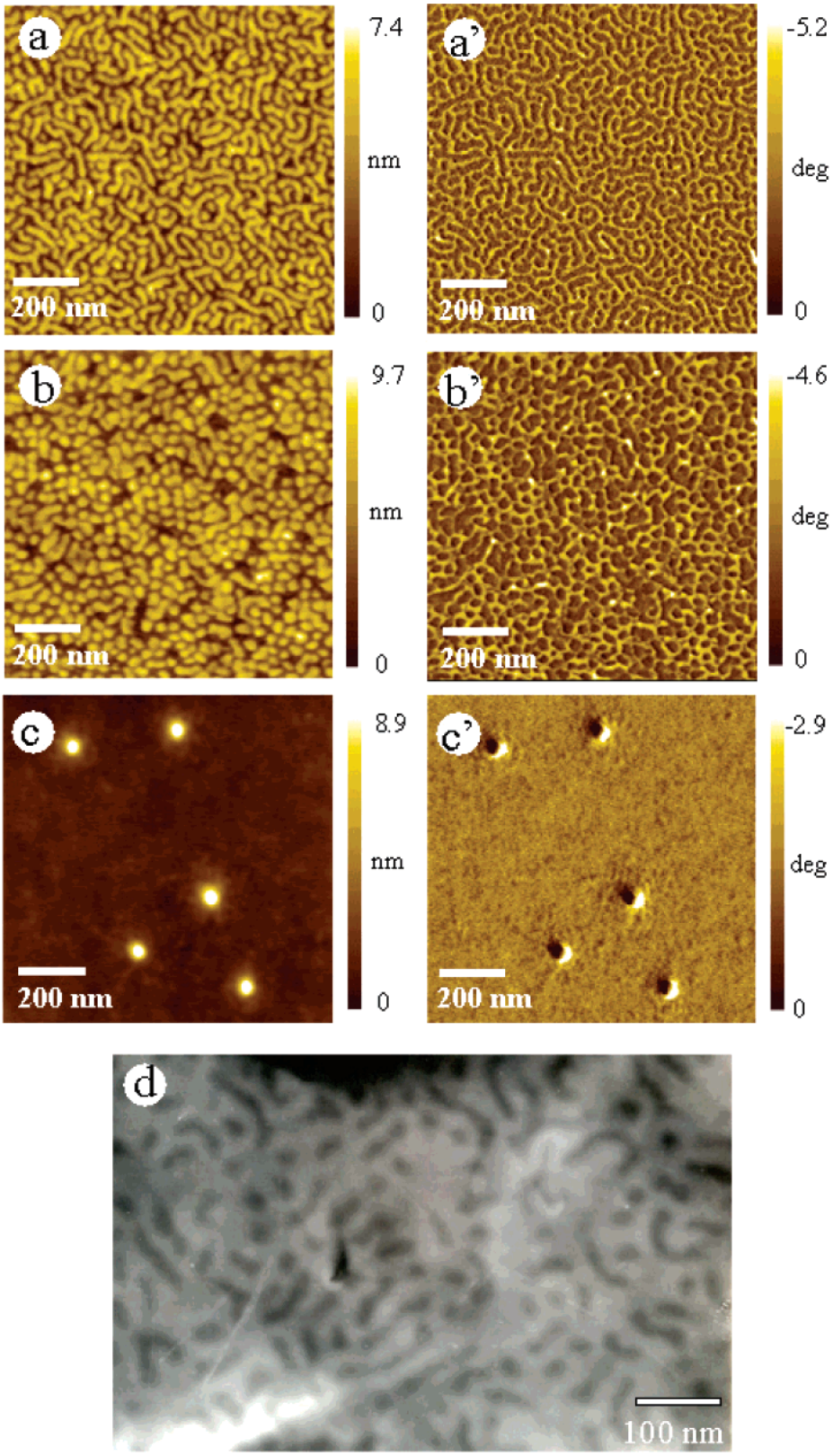

Figure 4. Tapping mode AFM height (a−c) and phase (a′−c′) images of copolymer **2** films spin-coated from (a,a′) 0.7 wt %, (b,b′) 0.5 wt %, and (c,c′) 0.1 wt % cyclohexanone solutions. (d) The corresponding plain-view bright-field TEM micrograph of (a).

unstained sample. The difference in the electron density between the PEG and PS phase provides good contrast in the bright-field TEM image. The PEG phase with higher electron density appears as dark domains, while the PS phase with lower electron density appears bright.

Such an effect of the concentration on the morphologies from the solutions can be understood by considering the concentration dependence of the χ_{P-S}. Normally, the χ_{P-S} dependence on the solution concentration could be positive, negative, or negligible.[36] As the concentration decreases, it is likely that the difference $\Delta\chi$ ($= |\chi_{PS-cyclo} - \chi_{PEG-cyclo}|$) decreases. So with the decreasing concentration, the wormlike pattern of copolymer **1** (Figure 3a,a′) became fuzzy (Figure 3b,b′) and finally

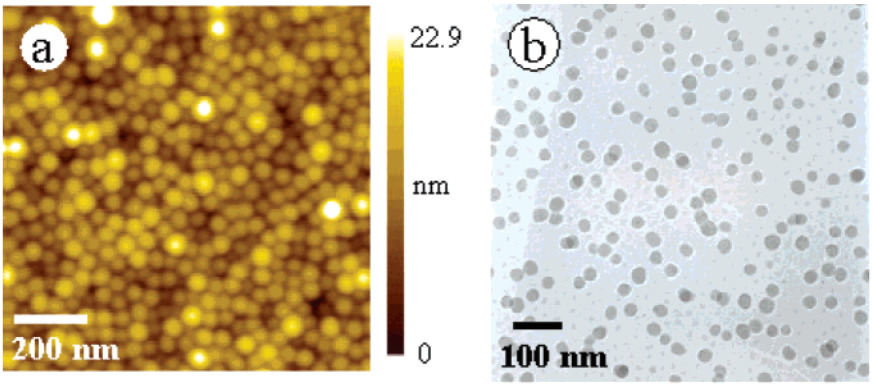

Figure 5. (a) Tapping mode AFM height image of copolymer **2** film spin-coated from 0.5 wt % acetonitrile solution. (b) TEM micrograph of copolymer **2** micelles in 0.2 wt % acetonitrile.

decomposed into spheres and unimers (Figure 3c,c′). This concentration dependence indicates the decrease in the solvent affinity between the PS and PEG blocks with the decreasing concentration. The trend of the copolymer chains to associate is largely depressed. Similarly, for copolymer **2**, the transition from PEG cylinders (Figure 4a) to PEG spheres (Figure 4b) and sphere/unimers (Figure 4c) is a clear indication of the decrease in the segregation strength and the association number.

3.1.3. Comparing the Effects of PS- and PEG-Affinitive Solvents on the Film Morphologies. In the same solution concentration (e.g., 0.5 wt %), it can be seen that the difference of solvent affinity influenced the surface morphology remarkably, i.e., the disordered state of the copolymer **1** films from PS-affinitive solvents (Figure 1) was transformed into wormlike cylinders from PEG-affinitive solvent (Figure 3a), and correspondingly, the PEG cylinders of the copolymer **2** films (Figure 2) were transformed into PEG spheres (Figure 4b). Normally, for the block copolymers (for example A−B diblocks) in dilute solutions of nominally neutral solvents, the solvent-affinitive block (e.g., A) will be more swollen while the other (e.g., B) will be less swollen.[40] Loose associates of the copolymer chains could be expected.[41−43] For the H-shaped copolymers here, however, such difference in the swelling degree may be not large enough to counteract the large volume difference between the PS and PEG blocks. Therefore, although the PEG blocks are preferentially swollen by cyclohexanone, the PS branches can also adopt an extending conformation so as to act as the matrix in the films. The swelling of the PEG blocks has the direct effect that the stretching of the PS branches could be relaxed, given that the aggregation number remained constant. The swelling of the PEG backbone chains contributes the penalty of entropy of the stretching of the PS branches. Thus, it is possible for copolymer **1** to achieve the disorder (Figure 1) to order (Figure 3a) transition, and for copolymer **2**, the PEG cylinders in a PS matrix (Figure 2) are transformed into PEG spheres in a PS matrix (Figure 4b).

3.2. Self-Assembly in PEG-Selective Solvent. 3.2.1. Spherical Micelles of Copolymer 2. In acetonitrile, a selective solvent for PEG and poor solvent for PS, copolymer **2** formed spherical micelles with PS cores and PEG coronas (Figure 5a) at room temperature. The spherical micelles have a uniform diameter of ∼25 nm (determined from the height of the micelle). These micelles are very stable even though we changed the solution concentration (e.g., 0.05, 0.2, and 1 wt %), increased the temperature up to 100 °C (above T_g^{PS}), or aged the micellar solutions at temperatures below T_m^{PEG} for long times. For example, the TEM image of the micelles prepared at 100 °C shows spheres of ∼25 ± 5 nm diameter (Figure 5b). Therefore, it is reasonable to conclude that copolymer **2** formed equilibrium spherical micelles in acetonitrile solutions, with PS cores and PEG coronas.

3.2.2. Mixed Spheres and Cylinders of Copolymer 1. At room temperature, copolymer **1** cannot dissolve in acetonitrile since the insoluble glassy PS blocks are much larger than the soluble PEG blocks. Micellar solutions can be obtained by dissolving the copolymer **1** powders at 100 °C. Then the solutions were quenched to ice bath temperature and stored at 10 °C for different times. The obtained solutions are transparent and stable upon long time storage.

Figure 6 shows the AFM height images of the films spin-coated from the 0.2 wt % micellar solution onto silicon wafers after storage at 10 °C for 1 h. A lot of cylinders with a length of several micrometers are observed (Figure 6a). The corresponding zoom-in images reveal that these cylinders can be normal continuous cylinders (Figure 6c) or aggregates of very short sinuate/branched nanorods that are arranged as long strands (Figure 6b). These cylinders and nanorods coexist with many spheres, and a lot of copolymer unimers exist on the background (Figure 6, parts b and c). In the AFM height images, the relative heights of these cylinders and spheres are approximately taken as the diameter, instead of the lateral dimension, due to the tip convolution effect. Accordingly, the average diameter of the cylinders is 11 nm. On the other hand, the average diameters of the nanorods and the spheres (except the unimers) are about 8 nm.

As the solution was aged at 10 °C for 1 day, the nanorods became longer and the branched structure was depressed (Figure 7a). Besides, the normal cylinders are also observed. After very long time aging (e.g., 11 days), the cylindrical assemblies are also obtained (Figure 7b). However, most of the cylinders appear as necklace-like strands of spheres and nanorods (Figure 7b inset), although the normal continuous cylinders can also be found. The TEM image verifies the self-assembled spheres and cylinders of copolymer **1** in acetonitrile solutions, where the unimers are invisible under the electron beam (Figure 7c). The cylinders have an average diameter of ∼11 nm, in good accordance with the AFM value. These morphological transitions may indicate some dynamic process of the self-assemblies in the PEG-selective solvent.

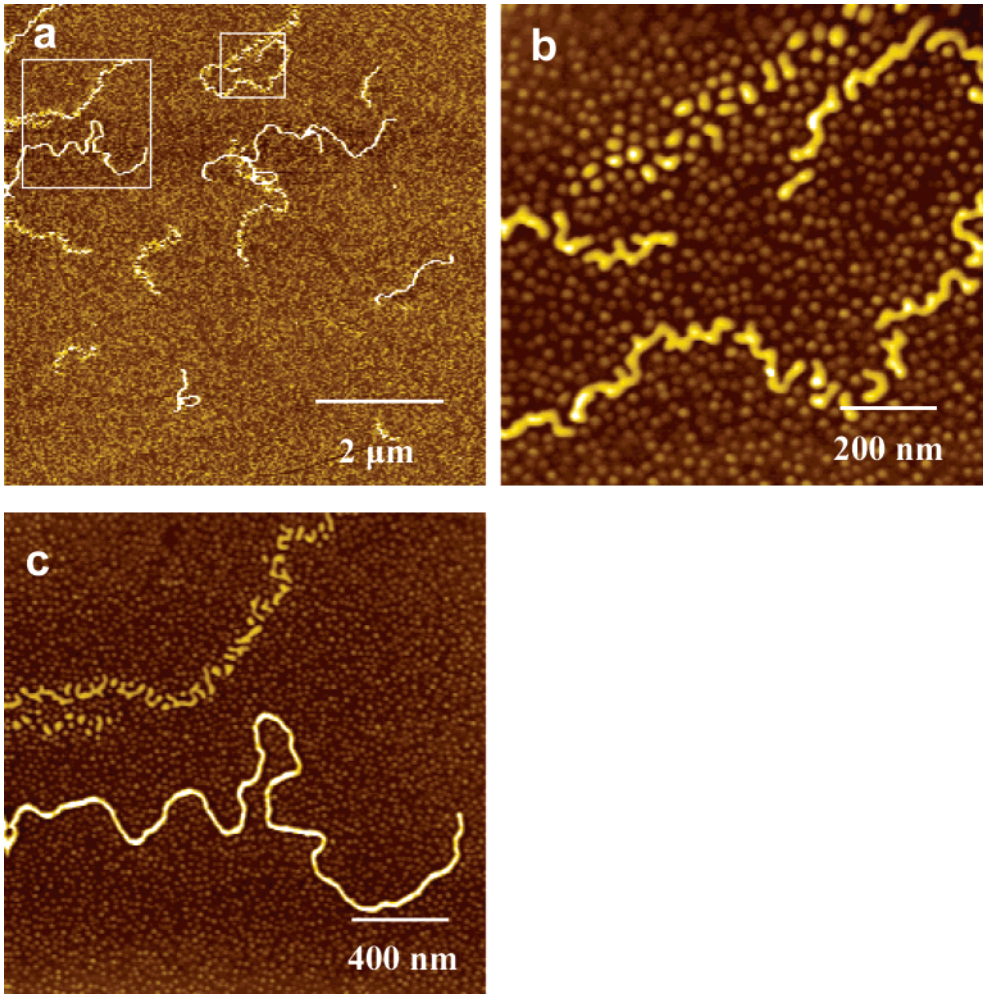

Figure 6. (a) AFM height image of the copolymer **1** aggregates from 0.2 wt % acetonitrile after aging for 1 h. (b) and (c) are the zoom-in images of the white squares, showing the detailed structures of the aggregates.

Normally, the geometry of the micelles depends on the interplay of the chain stretching in the core, the chain repulsion in the corona, and the solvent−core interfacial energy.[44,45] In our case, the H-shaped copolymer must have very strong repulsion between the PS branches. For the micelles formed in the PEG-selective solvent, there will be very strong stress inside the PS cores. Such stress can be largely relaxed by increasing the micelle size. However, more stretching of the chains is forced in order to reduce the unfavorable PS−acetonitrile contact. The balance of these two effects may favor the formation of cylinders, in which the PS branches can be more relaxed than in spheres.[44,45] In this context, it seems reasonable to take the spheres, nanorods, and cylinders as starting, intermediate, and stable assemblies in the solvent. According to the AFM images shown in Figures 6 and 7, all of these three structures exhibit stability and some dynamic equilibrium under the experimental conditions. This may be because the aging temperature is much lower than T_g^{PS}. Besides, the formation of the PEG loop in the corona may have an additional constraint to the transition from spheres to nanorods and cylinders.

3.2.3. Copolymer 1 Vesicles and Lamellae. As the copolymer **1**/acetonitrile solution concentration went down to 0.05 wt % at 100 °C, vesicles were obtained (Figure 8a). These vesicles seemed stable during aging at 10 °C for 2.5 days. After further aging to 8 days, however, the vesicles started to break (Figure 8b) and finally transformed into lamellae after aging for 50 days (Figure 8c).

Normally, dilution can induce a transition from vesicles or a bilayer structure to spherical micelles of block copolymers. Recently, Hu et al.[46] reported a morphological transition from spheres to vesicles upon diluting the micellar solution of the block copolymer/surfactant complexes. In principle, the transition from spheres to cylinders and vesicles can be induced by an increase in the solvent selectivity,[44,45] which favors the growth of the micelles. As the aggregation number per spherical micelle increases, the chains in the core and corona will be highly stretched. Therefore, the spherical micelles will transform into cylinders and/or vesicles in order to relax the copolymer chains.

In our case, it is not clear whether the solvent selectivity is significantly enhanced upon dilution. However, we can learn something from the transition to understand this abnormal behavior of this H-shaped copolymer with very low fraction of the soluble block. Comparing the transformation kinetics of these vesicles and that of the spheres and cylinders in Figures 6 and 7, one can conclude that these vesicles are more stable than the spheres and cylinders. This implies that the copolymer chains are more relaxed in these vesicles. The slow fracture of the vesicle took place at the edge of the vesicles (Figure 8b), indicating some internal stress inside the copolymer bilayer of the vesicles. Finally, the vesicles completely break into lamellae, with the inter-

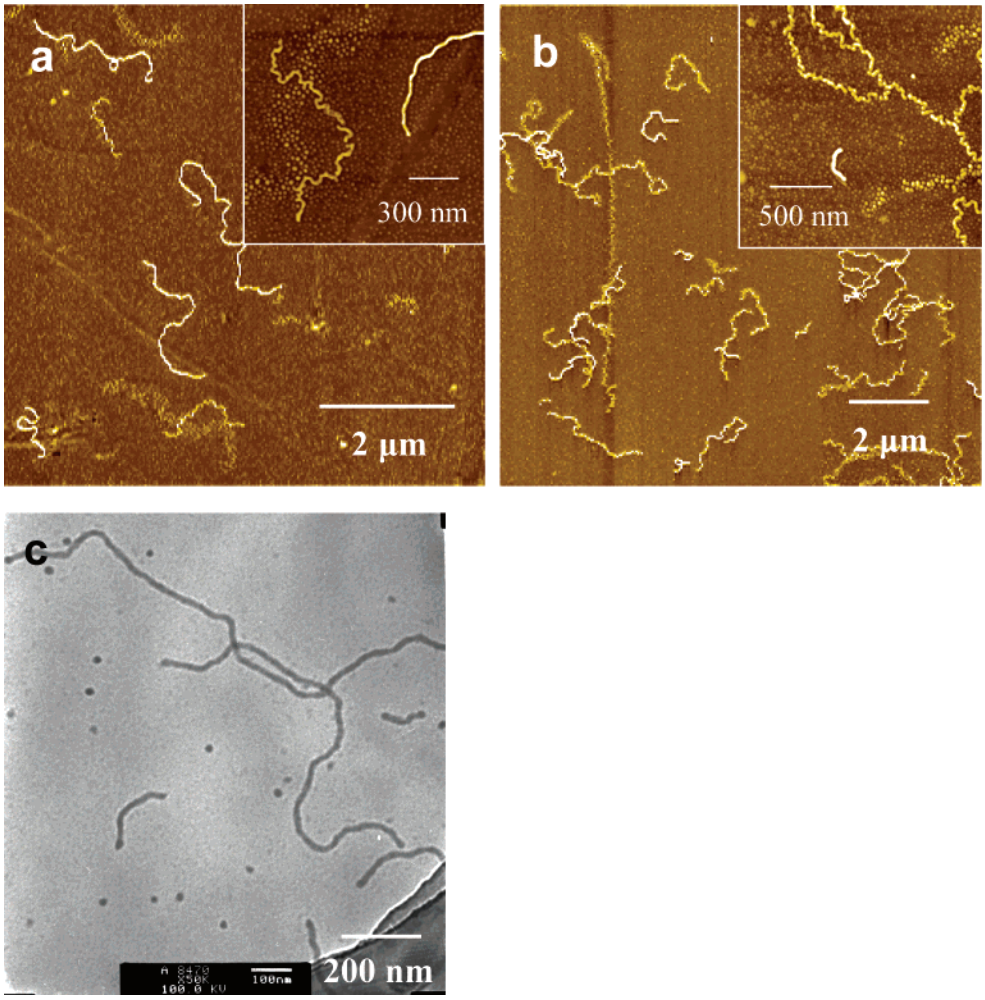

Figure 7. AFM height images of the copolymer **1** aggregates from 0.2% micellar solution aged for (a) 1 day and (b) 11 days. The insets show the corresponding detailed structure of the assemblies. (c) The corresponding plain-view bright-field TEM image of (b).

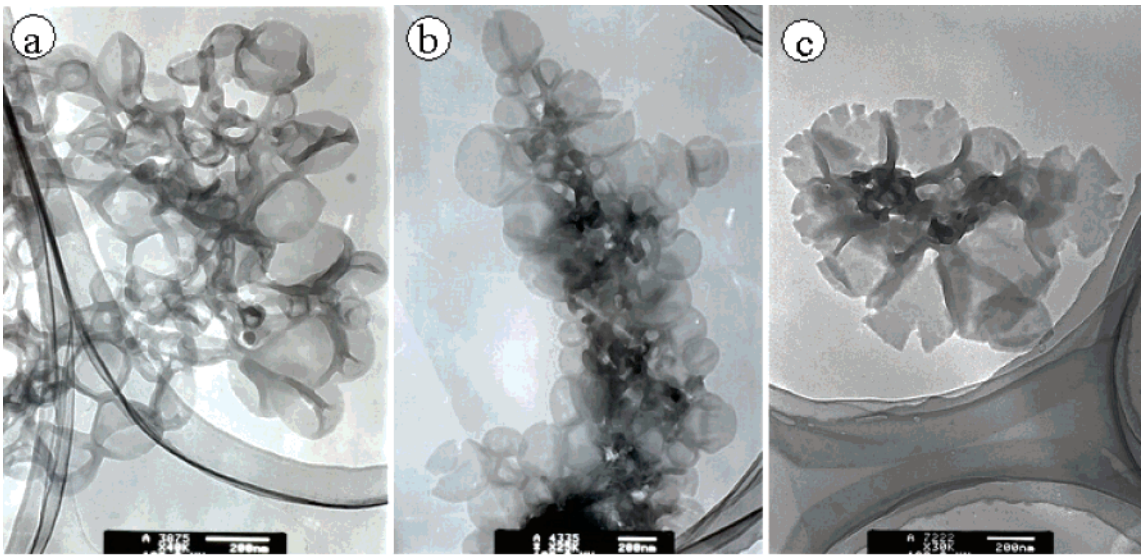

Figure 8. TEM micrographs of the aggregates morphologies of copolymer **1** in 0.05 wt % acetonitrile after aging for (a) 2.5 days, (b) 8 days, and (c) 50 days.

nal stress totally relaxed so that the lamellae are stable even upon aging for 5 months.

The internal stress may root from the specific architecture and the low PEG volume fraction. In the PEG-selective solvent, the micelles are composed of PS cores and PEG coronas. The very short PEG backbones require a highly compact packing of the highly stretched PS branches in the cores. Thus, the spheres are most unstable because of the strong repulsion between the PS chains in the cores; cylinders and vesicles are

favorable because they permit relaxation of the polymer chains. It seems that there is no curvature in the lamellae, which permits the most relaxed conformation of the copolymer chains and thus is the most stable geometry for the copolymer **1** in PEG-selective solvents.

4. Conclusions

The self-assembly of H-shaped block copolymers, i.e., $(PS)_2PEG(PS)_2$, in dilute solutions has been investigated, using both nominally neutral and PEG-selective solvents.

The nominally neutral solvents normally show slightly preferential affinity to a specific polymer according to the calculation of the polymer−solvent interaction parameter χ. Such solvent affinity (characterized by $\Delta\chi$) can remarkably influence the morphologies of spin-coated thin films of the copolymers. In the PS-affinitive solvents, the low-molecular-weight copolymer **1** films are in a disordered state. In contrast, the high-molecular-weight copolymer **2** formed randomly arranged wormlike patterns at the film surface. The phase separation strength of copolymer **2** in the solutions can be enhanced by very subtle increase in $\Delta\chi$. In the PEG-affinitive solvent (cyclohexanone), the $\Delta\chi$ value slightly decreases with the decreasing solution concentration. The separation strength of both copolymers was depressed so that the wormlike patterns of the copolymers were transformed into spheres coexisting with unimers.

In the PEG-selective solvent (acetonitrile), copolymer **2** formed equilibrium spherical micelles with PS cores and PEG coronas. At 100 °C, copolymer **1** formed micellar solutions, with a stable mixture of spheres and cylinders after quenching to 10 °C. Such micellar solutions are in a dynamic equilibrium state since the reversible transformation between the spheres, cylinders, and some intermediate micelles have been observed. These copolymer **1** micelles can be transformed into vesicles by diluting the solution. However, the vesicles are unstable and liable to break and finally transform into lamellae. Such morphology transformation may root from the high repulsion between the crowded PS chains in the cores due to the special architecture of the H-shaped copolymers and the very low volume fraction of the PEG blocks.

Acknowledgment. This work is subsidized by the National Natural Science Foundation of China (50125311, 20334010, 20274050, 50390090, 50373041, 20490220, 20474065, 50403007, 50573077), the Ministry of Science and Technology of China (2003CB615601), the Chinese Academy of Sciences (Distinguished Talents Program, KJCX2-SW-H07), and the Jilin Distinguished Young Scholars Program (20010101).

References and Notes

(1) Huang, H.; Hu, Z.; Chen, Y.; Zhang, F.; Gong, Y.; He, T. *Macromolecules* **2004**, *37*, 6523.
(2) Helfand, E.; Tagami, Y. *J. Chem. Phys.* **1972**, *56*, 3592.
(3) (a) Lodge, T. P.; Xu, X.; Ryu, C. Y.; Hamley, I. W.; Fairclough, J. P. A.; Ryan, A. J.; Pedersen, J. S. *Macromolecules* **1996**, *29*, 5955. (b) Lodge, T. P.; Hamersky, M. W.; Hanley, K. J.; Huang, C. I. *Macromolecules* **1997**, *301*, 6139. (c) Lodge, T. P.; Pudil, B.; Hanley, K. J. *Macromolecules* **2002**, *35*, 4707. (d) Lodge, T. P.; Hanley, K. J.; Pudil, B.; Alahapperuma, V. *Macromolecules* **2003**, *36*, 816.
(4) (a) Riess, G. *Prog. Polym. Sci.* **2003**, *28*, 1107. (b) Förster, S.; Plantenberg, T. *Angew. Chem., Int. Ed.* **2002**, *41*, 688. (c) Förster, S.; Antonietti, M. *Adv. Mater.* **1998**, *10*, 195. (d) Svenson, M.; Alexandridis, P.; Linse, P. *Macromolecules* **1999**, *32*, 637. (e) Pépin, M. P.; Whitmore, M. D. *Macromolecules* **2000**, *33*, 8644. (f) Kim, S. H.; Jo, W. H. *Macromolecules* **2001**, *34*, 7210.
(5) (a) Zhang, L.; Eisenberg, A. *Macromolecules* **1999**, *32*, 2239. (b) Shen, H.; Eisenberg, A. *Macromolecules* **2000**, *33*, 2561.
(6) (a) Yu, K.; Zhang, L.; Eisenberg, A. *Langmuir* **1996**, *12*, 5980. (b) Svensson, M.; Alexandridis, P.; Linse, P. *Macromolecules* **1999**, *32*, 5435. (c) Svensson, B.; Olsson, U.; Alexandridis, P. *Langmuir* **2000**, *16*, 6839.
(7) (a) Yu, K.; Eisenberg, A. *Macromolecules* **1996**, *29*, 6359. (b) Yu, K.; Eisenberg, A. *Macromolecules* **1998**, *31*, 3509.
(8) (a) Choucair, A.; Eisenberg, A. *Eur. Phys. J. E:* **2003**, *10*, 37. (b) Choucair, A.; Lavigueur, C.; Eisenberg, A. *Langmuir* **2004**, *20*, 3894. (c) Yu, Y.; Eisenberg, A. *J. Am. Chem. Soc.* **1997**, *119*, 8383.
(9) Schillén, K.; Brown, W.; Johnsen, M. *Macromolecules* **1994**, *27*, 4825.
(10) Raez, J.; Manners, I.; Winnik, M. A. *J. Am. Chem. Soc.* **2002**, *124*, 10381.
(11) Desbaumes, L.; Eisenberg, A. *Langmuir* **1999**, *15*, 36.
(12) (a) Zhang, L.; Shen, H.; Eisenberg, A. *Macromolecules* **1997**, *30*, 1001. (b) Kabanov, A.; Bronich, T. K.; Kabanov, V. A.; Eisenberg, A. *J. Am. Chem. Soc*. **1998**, *120*, 9941. (c) Zheng, Y.; Davis, H. T. *Langmuir* **2000**, *16*, 6453. (d) Borisov, O. V.; Zhulina, E. B. *Macromolecules* **2002**, *35*, 4472. (e) Ouarti, N.; Viville, P.; Lazzaroni, R.; Minatti, E.; Schappacher, M.; Deffieux, A.; Borsali, R. *Langmuir* **2005**, *21*, 1180.
(13) (a) Bi, L. K.; Fetters, L. J. *Macromolecules* **1976**, *9*, 732. (b) Pennisi, R. W.; Fetters, L. J. *Macromolecules* **1988**, *21*, 1094. (c) Iatrou, H.; Hadjichristidis, N. *Macromolecules* **1992**, *25*, 4649. (d) Patten, T. E.; Matyjaszewski, K. *Adv. Mater.* **1998**, *10*, 901. (e) Coessens, V.; Pintauer, T.; Matyjaszewski, K. *Prog. Polym. Sci.* **2001**, *26*, 337. (f) Matyjaszewski, K.; Xia, J. *Chem. Rev.* **2001**, *101*, 2921.
(14) (a) Roos, S. G.; Müller, A. H. E.; Matyjaszewski, K. *Macromolecules* **1999**, *32*, 8331. (b) Mecerreyes, D.; Atthoff, B.; Boduch, K. A.; Trollsås, M.; Hedrick, J. L. *Macromolecules* **1999**, *32*, 5175. (c) Schappacher, M.; Putaux, J. L.; Lefebvre, C.; Deffieux, A. *J. Am. Chem. Soc.* **2005**, *127*, 2990.
(15) (a) Hadjichristidis, N.; Pispas, S.; Pitsikalis, M.; Iatrou, H.; Vlahos, C. *Adv. Polym. Sci.* **1999**, *142*, 71. (b) Baek, K.-Y.; Kamigaito, M.; Sawamoto, M. *Macromolecules* **2001**, *34*, 7629. (c) Feng, X. S.; Pan, C. Y. *Macromolecules* **2002**, *35*, 2084. (d) Du, J.-Z.; Chen, Y.-M. *Macromolecules* **2004**, *37*, 3588. (e) Peleshanko, S.; Jeong, J.; Shevchenko, V. V.; Genson, K. L.; Pikus, Y.; Ornatska, M.; Petrash, S.; Tsukruk, V. V. *Macromolecules* **2004**, *37*, 7497. (f) Xu, J.; Zubarev, E. R. *Angew. Chem., Int. Ed.* **2004**, *43*, 5491. (g) Mountrichas, G.; Mpiri, M.; Pispas, S. *Macromolecules* **2005**, *38*, 940.
(16) Kotani, Y.; Kamigaito, M.; Sawamoto, M. *Macromolecules* **1998**, *31*, 5582. (b) Lord, S. J.; Sheiko, S. S.; LaRue, I.; Lee, H.; Matyjaszewski, K. *Macromolecules* **2004**, *37*, 4235.
(17) (a) Haddleton, D. M.; Perrier, S.; Bon, S. A. F. *Macromolecules* **2000**, *33*, 8246. (b) Beers, K. L.; Gaynor, S. G.; Matyjaszewski, K. *Macromolecules* **1998**, *31*, 9413. (c) Radke, W.; Müller, A. H. E. *Macromolecules* **2005**, *38*, 3949.
(18) (a) Zhai, X.; Peleshanko, S.; Klimenko, N. S.; Genson, K. L.; Vaknin, D.; Vortman, M. Ya.; Shevchenko, V. V.; Tsukruk, V. V. *Macromolecules* **2003**, *36*, 3101. (b) Cho, B. K.; Jain, A.; Nieberle, J.; Mahajan, S.; Wiesner, U.; Gruner, S. M.; Türk, S.; Räder, H. J. *Macromolecules* **2004**, *37*, 4227.
(19) (a) Zhu, Y.; Gido, S. P.; Iatrou, H.; Hadjichristidis, N.; Mays, J. W. *Macromolecules* **2003**, *36*, 148. (b) Minatti, E.; Viville, P.; Borsali, R.; Schappacher, M.; Deffieux, A.; Lazzaroni, R. *Macromolecules* **2003**, *36*, 4125.
(20) Fu, G. D.; Phua, S. J.; Kang, E. T.; Neoh, K. G. *Macromolecules* **2005**, *38*, 2612.
(21) Gido, S. P.; Lee, C.; Pochan, D. J.; Pispas, S.; Mays, J. W.; Hadjichristidis, N. *Macromolecules* **1996**, *29*, 7022.
(22) Roovers, J.; Toporowski, P. M. *Macromolecules* **1981**, *14*, 1174.
(23) Hakiki, A.; Young, R. N.; Mcleish, T. C. B. *Macromolecules* **1996**, *29*, 3639.
(24) Perny, S.; Allgaier, J.; Cho, D.; Lee, W.; Chang, T. *Macromolecules* **2001**, *34*, 5408.
(25) Iatrou, H.; Avgeropoulos, A.; Hadjichristidis, N. *Macromolecules* **1994**, *27*, 6232.
(26) Roovers, J. *Macromolecules* **1984**, *17*, 1196.
(27) Mcleish, T. C. B.; Allgaier, J.; Bick, D. K.; Bishko, G.; Biswas, P.; Blackwell, R.; Blottière, B.; Clarke, N.; Gibbs, B.; Groves, D. J.; Hakiki, A.; Heenan, R. K.; Johnson, J. M.; Kant, R.; Read, D. J.; Young, R. N. *Macromolecules* **1999**, *32*, 6734.

(28) Heinrich, M.; Pyckhout-Hintzen, W.; Allgaier, J.; Richter, D.; Straube, E.; Read, D. J.; Mcleish, T. C. B.; Groves, D. J.; Blackwell, R. J.; Wiedenmann, A. *Macromolecules* **2002**, *35*, 6650.
(29) Heinrich, M.; Pyckhout-Hintzen, W.; Allgaier, J.; Richter, D.; Straube, E.; Mcleish, T. C. B.; Wiedenmann, A.; Blackwell, R. J.; Read, D. J. *Macromolecules* **2004**, *37*, 5054.
(30) Jabbarzadeh, A.; Atkinson, J. D.; Tanner, R. I. *Macromolecules* **2003**, *36*, 5020.
(31) Lee, C.; Gido, S. P.; Poulos, Y.; Hadjichristidis, N.; Tan, N. B.; Trevino, S. F.; Mays, J. W. *J. Chem. Phys.* **1997**, *107*, 6460.
(32) Iatrou, H.; Willner, L.; Hadjichristidis, N.; Halperin, A.; Richter, D. *Macromolecules* **1996**, *29*, 581.
(33) Pispas, S.; Hadjichristidis, N.; Mays, J. W. *Macromolecules* **1996**, *29*, 7378.
(34) Li, Y. G.; Shi, P. J.; Pan, C. Y. *Macromolecules* **2004**, *37*, 5190.
(35) Kubies, D.; Rypáček, F.; Kovářová, J.; Lidnický, F. *Biomaterials* **2000**, *21*, 529.
(36) Brandrup, J., Immergut, E. H., Grulke, E. A., Abe, A., Bloch, D. R., Eds. *Polymer Handbook*, 4th ed.; John Wiley & Sons: New York, 1999.
(37) Magonov, S. N.; Reneker, D. H. *Annu. Rev. Mater. Sci.* **1997**, *27*, 175.
(38) Zhu, L.; Cheng, S. Z. D.; Calhoun, B. H.; Ge, Q.; Quirk, R. P.; Thomas, E. L.; Hsiao, B. S.; Yeh, F.; Lotz, B. *Polymer* **2001**, *42*, 5829.
(39) Fu, J.; Luan, B.; Yu, X.; Cong, Y.; Li, J.; Pan, C.; Han, Y.; Yang, Y.; Li, B. *Macromolecules* **2004**, *37*, 976.
(40) Huang, C. I.; Chapman, B. R.; Lodge, T. P.; Balsara, N. P. *Macromolecules* **1998**, *31*, 9384.
(41) Miller-Chou, B. A.; Koenig, J. L. *Macromolecules* **2003**, *36*, 4851.
(42) Tsunashima, Y.; Suzuki, S. *J. Phys. Chem. B* **1999**, *103*, 8675.
(43) Quintana, J. R.; Hernáez, E.; Inchausti, I.; Katime, I. *J. Phys. Chem. B* **2000**, *104*, 1439.
(44) Zhang, L.; Eisenberg, A. *J. Am. Chem. Soc*. **1996**, *118*, 3168.
(45) Burke, S. E.; Eisenberg, A. *Langmuir* **2001**, *17*, 6705.
(46) Hu, Z.; Jonas, A. M.; Varshney, S. K.; Gohy, J.-F. *J. Am. Chem. Soc*. **2005**, *127*, 6526.

MA0515679